Article

Simultaneous Binding of *meso*-Tetrakis(*N*-methylpyridinium-4-yl)porphyrin and 4‘,6-Diamidino-2-phenylindole at the Minor Grooves of Poly(dA)·poly(dT) and Poly[d(A–T)]: Fluorescence Resonance Energy Transfer between DNA Bound Drugs

Biao Jin, Hyun Mee Lee, Young-Ae Lee, Jae Hong Ko, Cheol Kim, and Seog K. Kim

J. Am. Chem. Soc., **2005**, 127 (8), 2417-2424• DOI: 10.1021/ja044555w • Publication Date (Web): 04 February 2005

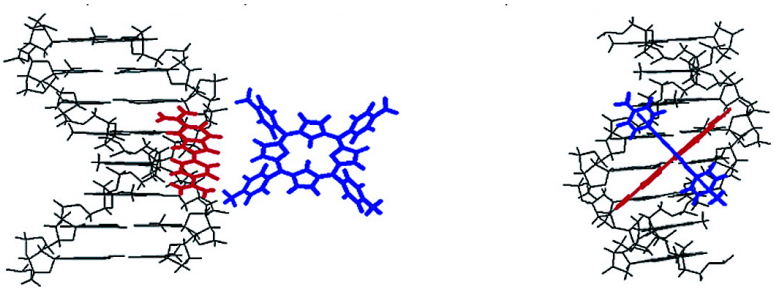

More About This Article

Additional resources and features associated with this article are available within the HTML version:

- Supporting Information
- Links to the 3 articles that cite this article, as of the time of this article download
- Access to high resolution figures
- Links to articles and content related to this article
- Copyright permission to reproduce figures and/or text from this article

View the Full Text HTML

J|A|C|S
ARTICLES
Published on Web 02/04/2005

Simultaneous Binding of *meso*-Tetrakis(*N*-methylpyridinium-4-yl)porphyrin and 4′,6-Diamidino-2-phenylindole at the Minor Grooves of Poly(dA)·poly(dT) and Poly[d(A−T)$_2$]: Fluorescence Resonance Energy Transfer between DNA Bound Drugs

Biao Jin,[†] Hyun Mee Lee,[†] Young-Ae Lee,[†] Jae Hong Ko,[†] Cheol Kim,[‡] and Seog K. Kim*,[†]

Contribution from the Department of Chemistry, Yeungnam University, 214-1 Dae-dong, Kyoungsan City, Kyoung-buk, 712-749, Republic of Korea, and Department of Fine Chemistry, Seoul National University of Technology, 172 Kongneung 2-dong, Seoul, 139-743, Republic of Korea

Received September 9, 2004; E-mail: seogkim@yumail.ac.kr

Abstract: The spectral properties of *meso*-tetrakis(*N*-methylpyridinium-4-yl)porphyrin (TMPyP) bound to poly(dA)·poly(dT) and poly[d(A−T)$_2$] in the presence and in the absence of 4′,6-diamidino-2-phenylindole (DAPI) have been studied. DAPI fits deeply into the minor groove of both poly(dA)·poly(dT) and poly[d(A−T)$_2$], and TMPyP is also situated at the minor groove. The nature of the absorption, circular dichroism (CD), and flow linear dichroism (LD) spectra of the TMPyP−poly(dA)·poly(dT) and −poly[d(A−T)$_2$] complexes in the Soret band is essentially unaffected whether the minor groove is blocked by DAPI or not, although small variations been noticed in the presence of DAPI. Furthermore, a close analysis of the reduced LD spectrum in the Soret band results in angles of ∼80° and 55° between transition moments of the TMPyP and DNA helix axes in the absence of DAPI. All these observations indicate that the side of TMPyP whose structure resembles that of classical minor groove binding drugs does not fit deeply into the minor groove. This suggests that TMPyP binds across the minor groove: two positively charged pyridiniumyl rings interact electrostatically with negatively charged phosphate groups of DNA. When DAPI and TMPyP are simultaneously bound to poly(dA)·poly(dT) or poly[d(A−T)$_2$], the fluorescence intensity of DAPI decreases as TMPyP concentration increases, indicating that the excited energy of DAPI is transferred to TMPyP.

Introduction

The interaction between DNA and porphyrin derivatives has been studied intensively for its potential application in photodynamic therapy, for example, and for its unique physicochemical properties in the interaction with nucleic acids.[1] The importance of this study was highlighted by the finding of the porphyrin derivatives' action as antiviral[2] and anticancer drugs.[3]

Water-soluble cationic porphyrin has been known to exhibit various modes of binding to DNAs. The structures of these porphyrin−DNA complexes have been extensively characterized using a variety of physical techniques, including NMR, equilibrium dialysis, circular and linear dichroism (CD and LD), and viscometry measurements.[1] For instance, *meso*-tetrakis(*N*-methylpyridinium-4-yl)porphyrin (referred to as TMPyP, Figure 1), a representative of this family, intercalates between the GC base pairs.[4,5] When associated with natural or AT-rich synthetic DNA, it exhibits various binding modes: TMPyP prefers to stack or to form an assembly along the AT-rich DNA at a high [porphyrin]/[DNA] ratio,[6] while it binds at the groove of AT sequences at a low [porphyrin]/[DNA] ratio.[7] Stacked or assembled TMPyP, which exhibits a bisignate induced CD spectrum in the Soret absorption band, occurs in the major groove.[8,9] In contrast, porphyrins that bind at the groove produce a positive CD band in the same region.

It has been well-known that unfused hydrocarbons bind preferentially in the minor groove of the AT-rich region.[10] 4′,6-

[†] Yeungnam University.
[‡] Seoul National University of Technology.

(1) (a) Fiel, R. J. *J. Biomol. Struct. Dyn.* **1989**, *6*, 1259−1274. (b) Marzilli, L. G. *New J. Chem.* **1990**, *14*, 409−420. (c) Pasternack, R. F.; Gibbs, E. J. In *Metal Ions in Biological Systems*; Sigel, A., Sigel, H., Eds.; Marcel Dekker: New York, 1996; pp 367−397.
(2) (a) Levere, R. D.; Gong, Y. F.; Kappas, A.; Bucher, D. J.; Wormser, G. P.; Abraham, N. G. *Proc. Natl. Acad. Sci. U. S. A.* **1991**, *88*, 1756−1759. (b) Ding, L.; Balzarini, J.; Schols, D.; Meunier, B.; de Clercq, E. *Biochem. Pharmacol.* **1992**, *44*, 1675−1679. (c) Pitie, M.; Casas, C.; Lacey, C.; Pratviel, J.; Bernadou, G.; Meunier, B. *Angew. Chem., Int. Ed. Engl.* **1993**, *32*, 557−559.
(3) Ding, L.; Etemad-Moghadam, G.; Cros, S.; Auclair, C.; Meunier, B. *J. Med. Chem.* **1991**, *34*, 900−906.
(4) (a) Marzilli, L. G.; Banville, L. D.; Wilson, W. D. *J. Am. Chem. Soc.* **1986**, *108*, 4188−4192. (b) Guliaev, A. B.; Leontis, N. B. *Biochemistry* **1999**, *38*, 15425−15437.
(5) Lee, Y.-A.; Lee, S.; Cho, T.-S.; Kim, C.; Han, S. W.; Kim, S. K. *J. Phys. Chem. B* **2002**, *106*, 11351−11355.
(6) (a) Marzilli, L. G. *New J. Chem.* **1990**, *14*, 409−420. (b) Lipscomb, L. A.; Zhou, F. X.; Presnell, S. R.; Woo, R. J.; Peek, M. E.; Plaskon, R. R.; Williams, L. D. *Biochemistry* **1996**, *35*, 2818−2823. (c) Ismail, M. A.; Rodger, P. M.; Rodger, A. *J. Biomol. Struct. Dyn.* **2000**, *Conversation 11*, 335−348. (d) Pasternack, R. F. *Chirality* **2003**, *15*, 329−332.

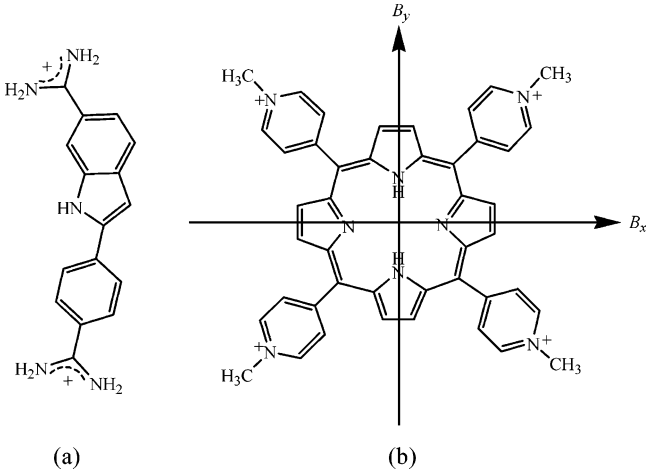

Figure 1. Molecular structures of (a) 4',6-diamidino-2-phenylindole and (b) *meso*-tetrakis(*N*-methylpyridium-4-yl)porphyrin.

Diamidino-2-phenylindole (referred to as DAPI, Figure 1) is one of the well-known examples.[11,12] The minor groove binding drugs possess common structural motifs—they adopt crescent shapes that match the turn of the helical motif in DNA. They also possess positive charges and a certain degree of rotational freedom for drugs to fit into the narrow minor groove. That TMPyP has a structural motif similar to those of conventional minor groove binding drugs makes TMPyP a possible candidate for a minor groove binding drug. Indeed, it was recently reported that the CD spectral properties of TMPyP associated with duplex $(dA)_n \cdot (dT)_n$ and triplex $(dA)_n \cdot [(dT)_n]_2$ at low binding ratios are similar, suggesting that the location of TMPyP is the minor groove.[8,9] Despite this possibility, it is not clear whether porphyrin fits deeply into the narrow minor groove or simply binds near or across the minor groove.

To clarify the binding mode of porphyrin at the groove of DNA, the spectral properties of TMPyP complexed with poly(dA)·poly(dT) and poly[d(A−T)$_2$] in the presence and in the absence of DAPI are compared in this study. The blocking of the minor groove by DAPI may alter the spectral properties of TMPyP if porphyrin fits deep into the minor groove. In addition, detailed analysis of the LD spectrum of the TMPyP−poly(dA)·poly(dT) and −poly[d(A−T)$_2$] complex is performed to determine the angle between the transition moments of the porphyrin molecule and the DNA helix axis.

Materials and Methods

Materials. All chemicals were purchased from Sigma and used without further purification. Poly(dA)·poly(dT) and poly[d(A−T)$_2$] were purchased from Amersham Biosciences Co. (Piscataway, NJ). The polynucleotides were dissolved in a 5 mM cacodylate buffer containing 1 mM EDTA and 100 mM NaCl at pH 7.0 and dialyzed several rounds against 50 mM NaCl, 5 mM cacodylate buffer, pH 7.0. The latter buffer was used throughout this work. The concentrations of the chemicals were determined spectrophotometrically using the following extinction coefficients: $\epsilon_{424\ nm} = 22\ 6000\ cm^{-1}\ M^{-1}$, $\epsilon_{342\ nm} = 27\ 000\ cm^{-1}\ M^{-1}$ for TMPyP and DAPI, respectively, and $\epsilon_{260\ nm} = 6000\ cm^{-1}\ M^{-1}$, $\epsilon_{262\ nm} = 6600\ cm^{-1}\ M^{-1}$ for poly(dA)·poly(dT) and poly[d(A−T)$_2$] in nucleic acid base, respectively. Samples were prepared by adding aliquots of concentrated porphyrin solution to appropriate DNA and DNA−DAPI solutions (typically up to 100 μL to 2 mL) before measurements, and the signals were corrected for volume changes. All measurements were performed at ambient temperature.

Polarized Light Spectroscopy. Drugs induce a CD spectrum upon binding to DNA, even though it does not possess a chiral center. The origin of this induced CD has been thought to be the interaction of the drug's electric transition moments with those of chirally arranged DNA bases. In the porphyrin−DNA complex case, various shapes of CD bands in the Soret absorption region have been known to represent porphyrin's characteristic binding modes. Stacked or extensively arrayed porphyrins on the DNA stem exhibit a characteristic bisignate CD due to the coupling of the oscillating dipoles between the DNA and porphyrin and/or of the porphyrin−porphyrin.[6,13] A negative CD band was observed for the porphyrins that intercalated between the GC base pairs,[5] while a positive CD was produced for the monomeric porphyrins that bind at or near the minor groove.[7−9]

LD is defined as the difference in absorbance by an oriented sample between the light polarized parallel ($A_{||}$) and perpendicular ($A_{\perp}$).[14] Measured LD is divided by isotropic absorption to give the reduced LD (LD^r), which is related to the angle, α, that specifies the orientation of the transition moment of drug relative to the local DNA helix:

$$LD^r = \frac{LD}{A} = \frac{A_{||} - A_{\perp}}{A} = \frac{3}{2}S(3\cos^2\alpha - 1)$$

where S is the orientation factor such that $S = 1$ for perfect orientation and $S = 0$ for random orientation. It can be calculated by assuming an angle of 86° between the $\pi \rightarrow \pi^*$ transition of the DNA base and the DNA helix axis.[15] Both CD and LD spectra were recorded on a Jasco J 715 polarimeter. For LD measurements, a flow-orienting Couette cell device with an inner rotating cylinder was used, as described by Nordén and Seth.[16] Polarized light spectra were averaged over several scans when necessary.

Absorption and Fluorescence Measurements. The fluorescence intensity of polynucleotide-bound DAPI decreases with increasing TMPyP concentration (see below). Quenching of the fluorescence may appear as a straight line in a Stern−Volmer plot if the quenching

(7) (a) Kuroda, R.; Tanaka, H. *J. Chem. Soc., Chem. Commun*. **1994**, 1575−1576. (b) Sehlstedt, U.; Kim, S. K.; Carter, P.; Goodisman, J.; Vollano, J. K.; Nordén, B.; Dabrowiak, J. C. *Biochemistry* **1994**, *33*, 417−426. (c) Schneider, H. J.; Wang, M. *J. Org. Chem*. **1994**, *59*, 7473−7478. (d) Yun, B. H.; Jeon, S. H.; Cho, T.-S.; Yi, Y.; Sehlstedt, U.; Kim, S. K. *Biophys. Chem*. **1998**, *70*, 1−10. (e) Lee, S.; Jeon, S. H.; Kim, B. J.; Han, S. W.; Jang, H. G.; Kim, S. K. *Biophys. Chem*. **2001**, *92*, 35−45. (f) Lee, S.; Lee, Y. A.; Lee, H. M.; Lee, J. Y.; Kim, D. H.; Kim, S. K. *Biophys. J*. **2002**, *83*, 371−381.
(8) Lee, Y.-A.; Kim, J.-O.; Cho, T.-S.; Song, R.; Kim, S. K. *J. Am. Chem. Soc*. **2003**, *125*, 8106−8107.
(9) Kim, J.-O.; Lee, Y.-A.; Yun, B. H.; Han, S. W.; Kwag, S. T.; Kim, S. K. *Biophys. J*. **2004**, *86*, 1012−1017.
(10) (a) Wilson, W. D. In *Nucleic Acids in Chemistry and Biology*; Blackburn, M., Gait, M., Eds.; Oxford Press: Oxford, U.K., 1990; pp 331−370. (b) Zimmer, C.; Wahnert, U. *Prog. Biophys. Mol. Biol*. **1986**, *47*, 37−112. (c) Warning, M. J. In *The Molecular Basis of Antibiotic Action*, 2nd ed.; Gale, E. F., Cundiffe, E., Reynolds, P. E., Richmond, M. H., Waring, M. J., Eds.; Wiley: New York, 1981; pp 287−292.
(11) (a) Nordén, B.; Erkisson, S.; Kim, S. K.; Kubista, M.; Lyng, R.; Åkerman, B. In *Molecular Basis of Specificity in Nucleic Acid-Drug Interactions*; Pullman, B., Jortner, J., Eds.; Kluwer Academic Publishers: Amsterdam, The Netherlands, 1990; pp 23−41. (b) Erkisson, S.; Kim, S. K.; Kubista, M.; Nordén, B. *Biochemistry* **1993**, *32*, 2987−2998. (c) Kim, H.-K.; Kim, J.-M.; Kim, S. K.; Rodger, A.; Nordén, B. *Biochemistry* **1996**, *35*, 1187−1194.
(12) (a) Larsen, T. A.; Goodsell, D. S.; Cascio, D.; Grzeskowiak, K.; Dickerson, R. E. *J. Biomol. Struct. Dyn*. **1989**, *7*, 477−491. (b) Mohan, S.; Yathindra, N. *J. Biomol. Struct. Dyn*. **1991**, *9*, 695−704. (c) Trotta, E.; D'Ambrosio, E.; Del Grosso, N.; Ravagnan, G.; Cirilli, M.; Paci, M. *J. Biol. Chem*. **1993**, *268*, 3944−3951. (d) Vlieghe, D.; Sponer, J.; Van Meervelt, L. *Biochemistry* **1999**, *38*, 16443−16451.
(13) (a) Pasternack, R. F.; Giannetto, A.; Pagano, P.; Gibbs, E. J. *J. Am. Chem. Soc*. **1991**, *113*, 7799−7800. (b) Pasternack, R. F.; Gibbs, E. J. *J. Inorg. Organomet. Polym*. **1993**, *3*, 77−88.
(14) (a) Nordén, B.; Kubista, M.; Kurucsev, T. *Q. Rev. Biophys. Chem*. **1992**, *25*, 51−170. (b) Nordén, B.; Kurucsev, T. *J. Mol. Recognit*. **1994**, *7*, 141−156. (c) Rodger, A.; Nordén, B. *Circular Dichroism & Linear Dichroism*; Oxford University Press: New York, 1997.
(15) (a) Matsuoka, Y.; Nordén, B. *Biopolymer* **1981**, *21*, 2433−2452. (b) Matsuoka, Y.; Nordén, B. *Biopolymer* **1982**, *22*, 1713−1734.
(16) Nordén, B.; Seth, S. *Appl. Spectrosc*. **1985**, *39*, 647−655.

mechanism follows either a simple static or a dynamic mechanism.[17]

$$F_0/F = 1 + K_{SV}[Q]$$

where K_{SV} is either the dynamic or static quenching constant and [Q] denotes the concentration of the quencher. However, an upward bending curve is often observed in the Stern−Volmer plot when the extent of quenching is large. Such positive deviations may be interpreted in terms of a "sphere of action", within which the probability of quenching is unity.

$$\frac{F_0}{F} = (1 + K_D[Q]) \exp([Q]VN/1000)$$

where $K_D = k_q\tau_0$ represents the dynamic quenching constant, with k_q and τ_0 being the bimolecular quenching constant and the fluorescence decay time in the absence of quencher, respectively. V is the volume of the sphere. The dynamic quenching efficiency, K_D, may be determined independently by measuring the fluorescence decay time in the absence and in the presence of the quencher. The fluorescence intensity of the DAPI−polynucleotides complex in the presence and in the absence of TMPyP was monitored at 370 and 460 nm, respectively, for excitation and emission. The slit widths were 8 and 12 nm, respectively. The steady-state fluorescence intensity of the DAPI−polynucleotide complex was measured at 360 and 456 nm for excitation and emission, respectively. The slit width was 5 nm for both excitation and emission.

Absorption spectra were recorded on a Cary 500 instrument and fluorescence on a Perkin-Elmer LS50B. Fluorescence decay times were measured using an IBH 5000U fluorescence lifetime system. The LED source of a nanoLED-03, which produces an excitation radiation at 370 nm with fwhm of ∼1.3 ns, was used to excite polynucleotide-bound DAPI.

Results

Absorption, CD, and LD Spectra. Binding of TMPyP to native and synthetic polynucleotides induces changes in the absorption spectrum in the Soret band. The extent of the red-shift and hypochromism or hyperchromism depends on the nature of polynucleotide, porphyrin, and the binding mode. Generally, the change is large for the intercalation and small for the groove binding or the stacking mode. The absorption spectra of the TMPyP−poly(dA)·poly(dT) and −poly[d(A−T)$_2$] complexes are depicted in Figure 2a and b, respectively, in the presence and in the absence of DAPI. The absorption spectra of the polynucleotide-bound DAPI and polynucleotide-free TMPyP are also presented for comparison. TMPyP exhibits 4% hyperchromism and a 6 nm red-shift upon binding to poly(dA)·poly(dT) compared to polynucleotide-free TMPyP, with its maximum being at 427 nm. In the presence of DAPI, no shift but a ∼10% decrease in absorbance at the absorption maximum is observed. Polynucleotide-free DAPI in aqueous solution exhibits an absorption maximum at ∼340 nm (data not shown), which shifts to longer wavelength by about 20 nm upon binding to the minor groove of DNA or AT-rich polynucleotides.[11] An absorption maximum around ∼360−370 nm is visible for the TMPyP−DAPI−poly(dA)·poly(dT) complex, suggesting that DAPI remains bound even in the presence of TMPyP. The absorption maximum of the TMPyP−poly(dA)·poly(dT) complex remains at 427 nm even when the minor groove is saturated by DAPI, although a small decrease in the absorbance was observed, suggesting that TMPyP also remains bound. A small decrease in absorbance may be explained by the change in the environment of TMPyP induced by the presence of DAPI. Changes in the absorption spectrum for the TMPyP−DAPI−poly[d(A−T)$_2$] system are similar to those of the TMPyP−poly(dA)·poly(dT) complex (Figure 2b), except that the TMPyP−poly[d(A−T)$_2$] complex exhibits a 9 nm red-shift and 4% hypochromism compared to that in the aqueous solution, leading to the same conclusion, i.e., TMPyP and DAPI can bind simultaneously to both AT-rich polynucleotides.

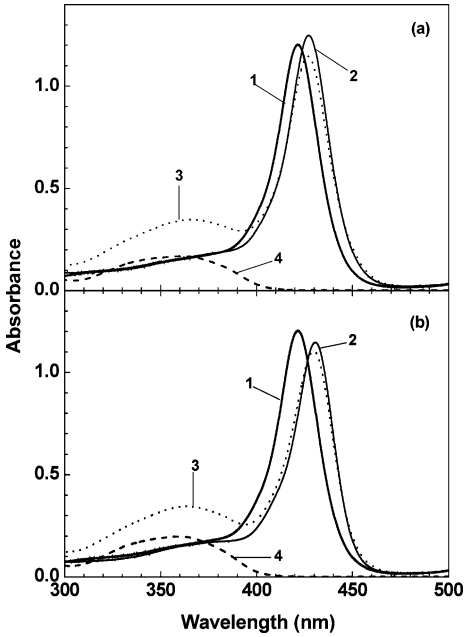

Figure 2. (a) Absorption spectrum of the DAPI−polyd(A)·poly(dT) (dashed curve, curve 4), TMPyP−polyd(A)·poly(dT) (solid curve, curve 2), and TMPyP−DAPI−polyd(A)·poly(dT) (dotted curve, curve 3) complexes. That of polynucleotide-free TMPyP is also shown for comparison (thick solid curve, curve 1). [TMPyP] = 5 μM, [DAPI] = 8 μM, and [polyd(A)·poly(dT)] = 100 μM in base. (b) Absorption spectrum of the TMPyP−DAPI−poly[d(A−T)$_2$] system. Concentrations and curve assignment are the same as in (a).

The CD spectrum in the Soret absorption region seems to be a good indicator of the binding mode of the porphyrin−DNA complex. As depicted in Figure 3a and b, the induced CD spectrum of TMPyP appeared to be positive in the Soret region when TMPyP was associated with poly(dA)·poly(dT) as well as with poly[d(A−T)$_2$], suggesting that the binding mode to these duplexes is similar, although the intensity is about 1.6 times higher for the complex with poly(dA)·poly(dT). The positive CD signal in the Soret absorption region for the TMPyP−polynucleotides complex may be explained by TMPyP being associated at the groove of DNA.[7−9] When DAPI is associated with both polynucleotides, an induced positive CD signal with its maximum at about 366 nm is apparent. A similar induced CD signal has been reported for the DAPI that bound to the minor groove of AT-rich DNA at a high binding density.[11] The CD spectrum of the TMPyP−DAPI−poly(dA)·poly(dT) complex shows positive signals at about 368 and 424 nm, respectively, corresponding to polynucleotide-bound DAPI and TMPyP, suggesting that both TMPyP and DAPI are simultaneously bound to poly(dA)·poly(dT). However, the CD spectrum of the TMPyP−DAPI−poly(dA)·poly(dT) complex is not identical to the sum of the spectra of the DAPI−poly(dA)·poly(dT)

(17) Lakowiz, J. R. *Principles of Fluorescence Spectroscopy*, 2nd ed.; Plenum Press: New York, 2001; pp 237−247.

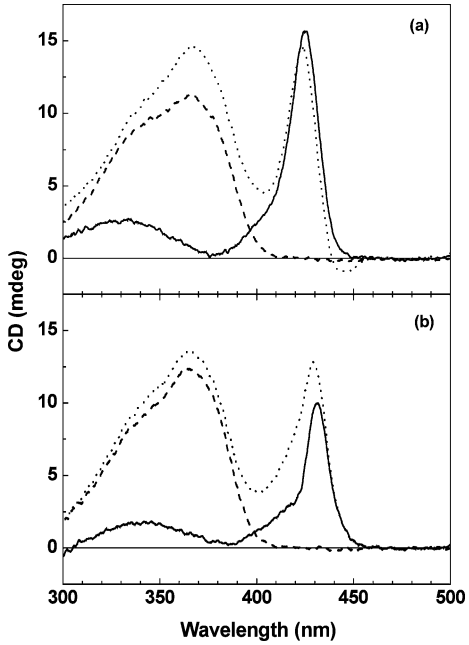

Figure 3. (a) CD spectrum of the TMPyP−poly(dA)·poly(dT) (solid curve), DAPI−poly(dA)·poly(dT) (dashed curve), and TMPyP−DAPI-poly(dA)·poly(dT) (dotted curve) complexes. (b) CD spectrum of the TMPyP−poly-[d(A−T)$_2$] (solid curve), DAPI−poly[d(A−T)$_2$] (dashed curve), and TMPyP−DAPI−poly[d(A−T)$_2$] (dotted curve) complexes. The concentrations are the same as in Figure 2a.

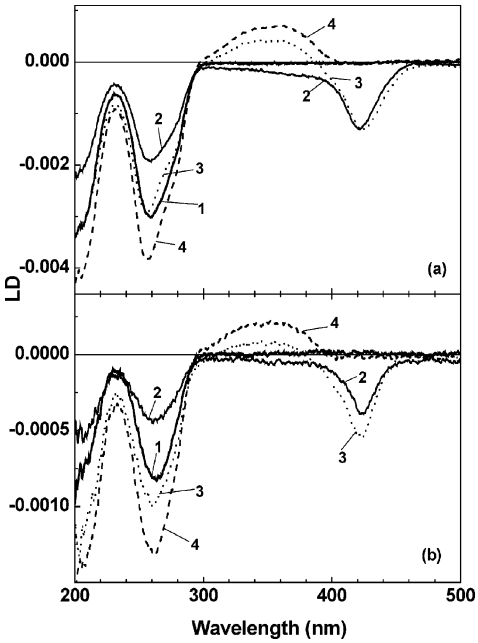

Figure 4. LD spectra of (a) the TMPyP−DAPI−polyd(A)·poly(dT) system and (b) the TMPyP−DAPI−polyd[d(A−T)$_2$] system. The curve assignments and the concentrations are the same as in Figure 2.

and TMPyP−poly(dA)·poly(dT) complexes, indicating that the local environment is changed for both drugs. A similar result is observed for the TMPyP−DAPI−poly[d(A−T)$_2$] system (Figure 3b). It is noteworthy that a decrease in the DAPI CD signal is apparent for the TMPyP−DAPI−poly(dA)·poly(dT) complex, while a decrease in the Soret region is observed for the TMPyP−DAPI−poly[d(A−T)$_2$] complex.

Figure 4a and b depicts the measured LD spectra for the TMPyP−DAPI−poly(dA)·poly(dT) and the TMPyP−DAPI−poly[d(A−T)$_2$] systems, respectively. Both drug-free poly(dA)·poly(dT) and poly[d(A−T)$_2$] exhibit negative LD signals in the DNA absorption region (curves 1), as expected from our LD system.[14−16] The difference in the magnitude of the measured LD value in the DNA absorption region (∼260 nm) can be attributed to the difference in the length and the flexibility of two polynucleotides. When TMPyP is bound, a significant decrease in the LD magnitude in the DNA absorption region is apparent for both polynucleotides (curves 2), suggesting that the binding of TMPyP results in a decrease in the orientability of the polynucleotide. Negative LD signals in the Soret region are also apparent for both complexes, excluding the possibility that the angle of both the B_x and B_y transitions relative to the DNA helix is 45°, which has been observed for the classical minor groove binding drugs. When DAPI is bound, an increase in the LD magnitude in the DNA absorption region and the positive LD in the DAPI absorption region are apparent for both the DAPI−poly(dA)·poly(dT) and the DAPI−poly[d(A−T)$_2$] complexes, as has been reported (curves 4).[11] A decrease in LD magnitude in the DAPI absorption region for both TMPyP−DAPI−poly(dA)·poly(dT) and TMPyP−DAPI−poly[d(A−T)$_2$] complexes and an increase in the Soret band for the latter complex are apparent.

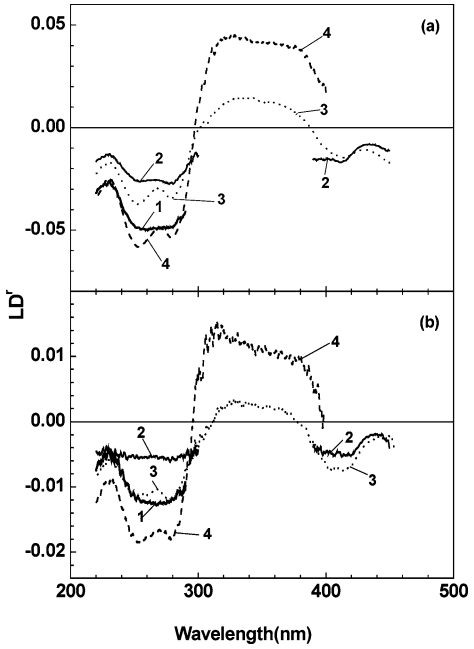

Figure 5. LD^r spectra of (a) the TMPyP−DAPI−polyd(A)·poly(dT) system and (b) the TMPyP−DAPI−polyd[d(A−T)$_2$] system. The curve assignments and the concentrations are the same as in Figure 2.

The appearance of the LD^r spectrum is directly related to the angle of the transition moment of the DNA-bound drug, in particular the B_x and B_y transitions in the porphyrin case, relative to the DNA helix axis. The LD^r spectra of the TMPyP−DAPI−poly(dA)·poly(dT) and TMPyP−DAPI−poly[d(A−T)$_2$] systems are shown in Figure 5a and b, respectively. In both the DAPI−poly(dA)·poly(dT) and the DAPI−poly[d(A−T)$_2$] complex cases (curves 4), a negative LD^r in the DNA absorption region with a small positive sign and a positive, relatively wavelength-independent LD^r signal is apparent. Angles of 40−44° are obtained for the two DAPI transitions, which coincide with known values,[11] in accordance with deep binding of DAPI in the minor groove. In the TMPyP−DAPI−polynucleotide com-

plexes cases, the magnitude of LD^r in the DAPI absorption region decreases. The angle between the DAPI transition moment and the DNA helix axis is 48−52° for both poly(dA)·poly(dT) and poly[d(A−T)$_2$]. A decrease in LD^r magnitude in the DNA absorption region upon binding of TMPyP to both poly(dA)·poly(dT) and poly[d(A−T)$_2$] (compare curves 1 and 2) and to DAPI−poly(dA)·poly(dT) and the DAPI−poly-[d(A−T)$_2$] complex (curves 4 and 3) indicates that binding of TMPyP results in a decrease in polynucleotide and DAPI−polynucleotide complex. In the Soret region, LD^r is strongly wavelength-dependent. The shape of LD^r is similar in the presence (curves 3) and in the absence (curves 2) of DAPI, suggesting that the geometry of TMPyP may be similar. The negative LD^r value in the Soret region excludes the possibility that both the B_x and B_y transitions of the porphyrin molecule orient near 45° relative to the DNA helix axis:[14−16] the orientation angle of 45° is typical for the minor groove binding drugs such as DAPI.[11] The LD^r signal in the Soret region strongly depends on the wavelength for both complexes in the presence and in the absence of DAPI, suggesting that the degeneracy of the B_x and B_y transitions is removed, i.e., the interaction of the transition moments with DNA is different or the binding mode of porphyrin to DNA is heterogeneous. It is noteworthy that the magnitude of LD^r in the DNA absorption region decreases for both TMPyP−poly(dA)·poly(dT) and TMPyP−poly[d(A−T)$_2$] complexes upon porphyrin binding compared to that in the absence of porphyrin, suggesting that the orientability of DNA decreased.

Analysis of LD^r Spectra of the TMPyP Complexed with Poly(dA)·Poly(dT) and Poly[d(A−T)$_2$]. The appearance of wavelength-dependent LD^r in the drug's absorption region indicates that two or more transition moments are involved in a given absorption band. Particularly, wavelength-dependent LD^r in the Soret region of the porphyrin−DNA complex implies that the degeneracy of the transition moments of porphyrin in the Soret band (B_x and B_y bands) is removed upon binding to DNA, by having different angles with respect to the DNA helix axis.[5] If this is the case, the LD^r spectrum may be analyzed by noticing that the absorption and LD spectra are the sums of contributions from the two transitions:[18,19]

$$A(\lambda) = t_1T_1(\lambda) + t_2T_2(\lambda)$$

$$\mathrm{LD}(\lambda) = t_3T_3(\lambda) + t_4T_4(\lambda)$$

where $T_1(\lambda)$ and $T_2(\lambda)$ are absorption profiles of the B_x and B_y transitions that contribute to the absorption spectrum, and $T_3(\lambda)$ and $T_4(\lambda)$ are those that contribute to the LD spectrum. The t_i's are the coefficients. The contribution of pure $T_2(\lambda)$ can be obtained by subtraction of the properly tuned LD spectrum, multiplied by a weighing factor (κ), from the measured absorption spectrum because the contributions of the two transition moments to absorption and LD spectra are different.

$$T_2(\lambda) = A(\lambda) - \kappa\mathrm{LD}(\lambda)$$

Figure 6a shows the $A(\lambda) - \kappa\mathrm{LD}(\lambda)$ spectrum of the TMPyP−poly(dA)·poly(dT) complex, with the κ ranges from −0.3 to −1.4 (from top to bottom) with an increment of −0.1. The measured absorption and LD spectra (multiplied by a factor of 100) are shown at the top and bottom of the figure, respectively. The absorption profile with $\kappa = -0.5$ (shown as a dashed curve in Figure 6a) was chosen as the best representative curve for the long-wavelength transition, $T_2(\lambda)$. Subtraction of $T_2(\lambda)$ from the measured absorption spectrum results in the absorption profile of the short-wavelength transition, $T_1(\lambda)$ (Figure 6b). Two absorption profiles obtained for the TMPyP−poly[d(A−T)$_2$] complex are shown in Figure 6c. The LD^r values for each transition moment can be calculated from the following expressions:[18,19]

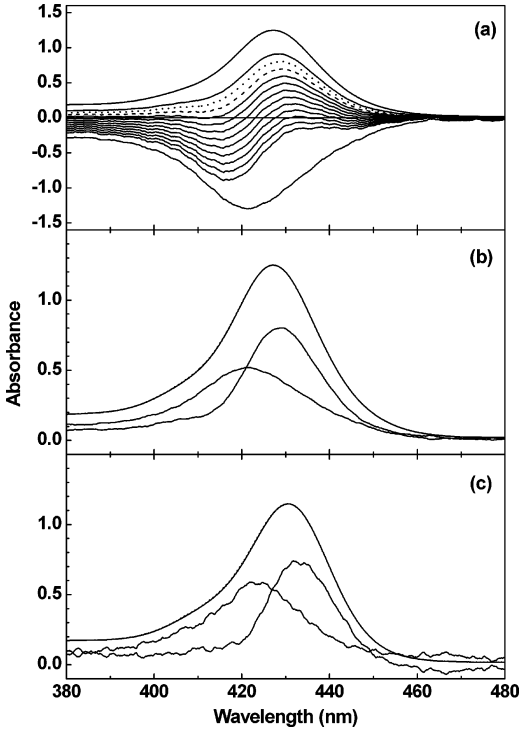

Figure 6. (a) The difference spectra, $A(\lambda) - \kappa\mathrm{LD}(\lambda)$, of TMPyP bound to poly(dA)·poly(dT) in the Soret region. [TMPyP] = 5 μM and [poly(dA)·poly(dT)] = 100 μM base. Top and bottom curves are absorption and LD (multiplied by a factor of 100), respectively. The κ value varied between −0.3 and −1.4 with an increment of −0.1. The dotted curve with κ = −0.4 is considered the most representative profile of the short-wavelength transition. (b) Absorption spectrum of the TMPyP−poly(dA)·poly(dT) complex resolved into the contributions from two transitions. (c) Absorption spectrum of the TMPyP−poly[d(A−T)$_2$] complex resolved into the contributions from two transitions by the same method as for the TMPyP-poly(dA)·poly(dT) complex.

$$\mathrm{LD}_1^{\mathrm{r}} = \frac{t_3}{t_1} \qquad \text{and} \qquad \mathrm{LD}_2^{\mathrm{r}} = \frac{t_4}{t_2}$$

Once LD^r values are obtained, the angle between each transition moment and the DNA helix axis can be calculated by assuming an angle of 86° between the plane of the DNA base and the DNA helix axis. A similar approach was reported for the TMPyP−poly[d(I−C)$_2$] complex.[5] Angles of 74° and 55° were obtained for the short- and long-wavelength transitions of both the TMPyP−poly(dA)·poly(dT) and TMPyP−poly[d(A−T)$_2$] complexes. Choosing the κ value, thereby, the representative

(18) (a) Kubista, M.; Åkerman, B.; Nordén, B. *Biochemistry* **1987**, *26*, 4545−4553. (b) Kim, S. K.; Eriksson, S.; Kubista, M.; Nordén, B. *J. Am. Chem. Soc.* **1993**, *115*, 3441−3447.

(19) Michl, J.; Thulstrup, E. W. *Spectroscopy with Polarized Light*; VCH Publidhing Inc.: Weinheim, Germany, 1986; p 423.

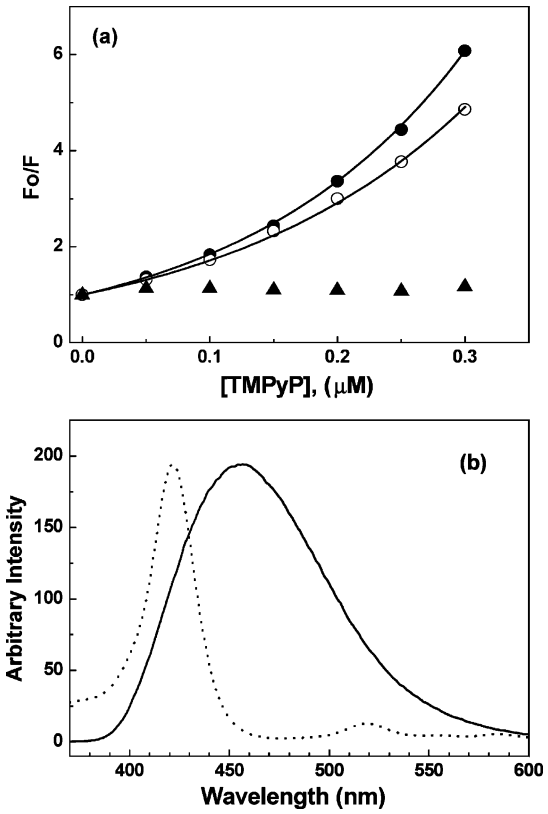

Figure 7. (a) Stern−Volmer plot for the fluorescence quenching of the DAPI−poly(dA)·poly(dT) (open circles) and DAPI−poly[d(A−T)$_2$] complexes (closed circles) by TMPyP. The solid curves are the best-fit curve for the equation $F_0/F = (1 + K_D[Q])\exp([Q]VN/1000)$ (see the text for the appropriate values of K_D and V). That in the absence of polynucleotide is shown as closed triangles. [Polynucleotide] = 10 μM, [DAPI] = 0.8 μM. Fluorescence intensities were read with the excitation at 360 nm and emission at 456 nm. Slit width was 5 nm for both excitation and emission. (b) Fluorescence emission spectrum of the DAPI−poly[d(A−T)$_2$] complex (excitation at 360 nm) and rescaled absorption spectrum of the TMPyP−poly[d(A−T)$_2$] complex.

absorption profiles for the transitions somewhat affect the resulting angle. For instance, when we choose $\kappa = -0.4$ (Figure 6a, dotted curve) instead of $\kappa = -0.5$, the resulting angles were 82° and 55°, and for $\kappa = -0.6$ (Figure 6a, dotted curve), the resulting angles were 70° and 55°. However, variation in the angles by these amounts did not affect our qualitative discussion; i.e., neither the intercalation mode nor classical minor groove binding mode of TMPyP can produce these angles.

Decrease in Fluorescence Intensity of the DAPI−Poly(dA)·Poly(dT) and −Poly[d(A−T)$_2$] Complexes upon TMPyP Binding. The fluorescence intensity of the DAPI−poly(dA)·poly(dT) and −poly[d(A−T)$_2$] complexes decreases with increasing TMPyP concentration. When the ratio of the fluorescence in the absence of TMPyP to that in the presence is plotted with respect to the TMPyP concentration (F_0/F versus [TMPyP], a normal Stern−Volmer plot),[17] upward-bending curves are observed for both the DAPI−poly[d(A−T)$_2$] and −poly(dA)·poly(dT) complexes (Figure 7a).The quenching efficiency of TMPyP for the DAPI−poly[d(A−T)$_2$] complex is slightly higher than that of the DAPI−poly(dA)·poly(dT) complex. It should be noted that in the absence of polynucleotide, no quenching activity is observed, ensuring that the fluorescence quenching of DAPI by TMPyP occurs only when they bind simultaneously to the polynucleotide. It should also be noted that the fluorescence of TMPyP at appropriate excitation and emission wavelengths for DAPI fluorescence (360 and 456 nm, respectively) is negligible. Therefore, the decrease in fluorescence intensity is certainly caused by the DAPI molecule. A large overlap between the emission band of the DAPI−polynucleotide complex and the absorption spectrum of the TMPyP is observable (Figure 7b), suggesting that the mechanism behind the decrease in DAPI fluorescence involves, at least in part, the resonance energy transfer type. If the fluorescence quenching is described by a "sphere of action" model, in which both static and dynamic mechanisms are involved, the Stern−Volmer plot can be modified to involve both mechanisms (see Materials and Methods). In the equation, the dynamic quenching constant may be obtained by independent measurement of the fluorescence decay time in the presence and in the absence of TMPyP (see below). Utilizing the K_D values of 1.21×10^6 M^{-1} for the TMPyP−DAPI-poly[d(A−T)$_2$] complex and 0.88×10^6 M^{-1} for the TMPyP−DAPI−poly(dA)·poly(dT) complex, sphere radii near 125 and 122 Å are obtained, respectively. These values are unrealistically large. Usually the sphere radius is in a range comparable to the sum of the radii of the fluorophore and quencher.[20] The dramatic effect on the extent of quenching may be attributed to the electronic charge on TMPyP. Considering the highly negatively charged DNA, quenching efficiency is expected to be sensitive to the charge of TMPyP and the rate of quencher diffusion near the DNA helix.[21]

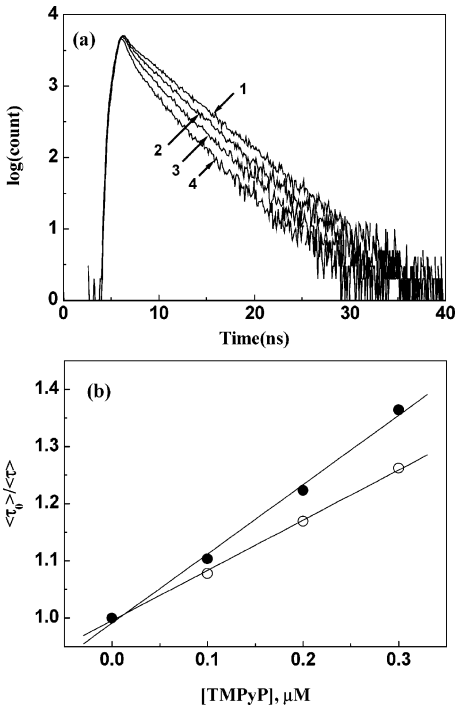

Figure 8. (a) Decay profile of the DAPI−poly[d(A−T)$_2$] complex in the absence (curve 1) and in the presence of TMPyP (curves 2−4). The concentrations of TMPyP were 0.1, 0.2, and 0.3 μM. The complex was excited at 370 nm by an LED source. The emission was detected at 460 nm. Slit widths were 8 and 12 nm for excitation and emission, respectively. [DAPI] = 0.8 μM, [polynucleotide] = 10 μM in base. (b) Ratio of average decay time (as defined in the text) of the DAPI−poly[d(A−T)$_2$] (closed circles) and DAPI−poly(dA)·poly(dT) (open circles) complexes in the absence of TMPyP to that in their presence.

(20) Casali, E.; Oetra, P. H.; Ross, J. B. A. *Biochemistry* **1990**, *29*, 9334−9343.
(21) Pasternack, R. F.; Caccam, M.; Keogh, B.; Stephenson, T. A.; Williams, A. P.; Gibbs, E. J. *J. Am. Chem. Soc.* **1991**, *113*, 6835−6840.

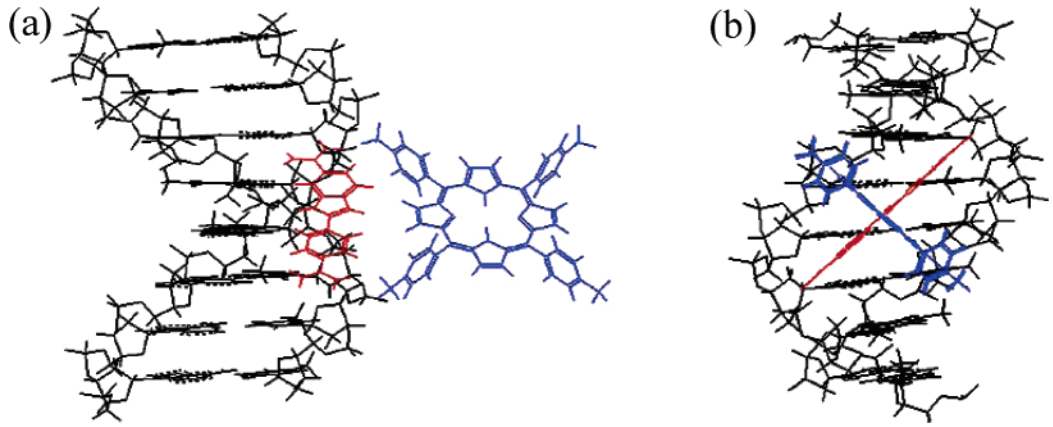

Figure 9. Illustration for the binding of TMPyP (blue) across the minor groove of DNA in the presence of DAPI (red).

The fluorescence decay times of both the DAPI−poly(dA)·poly(dT) and the DAPI−poly[d(A−T)$_2$] complexes are shortened by the presence of TMPyP. In the absence of TMPyP, the DAPI−poly[d(A−T)$_2$] complex exhibits two decay components, $\tau_1 = 0.44$ ns and $\tau_2 = 3.85$ ns, with their relative amplitudes $a_1 = 8.28\%$ and $a_2 = 91.72\%$, respectively (Figure 8a, curve 1). The decay components of the DAPI−poly(dA)·poly(dT) complex are $\tau_1 = 0.49$ ns ($a_1 = 7.53\%$) and $\tau_2 = 3.95$ ns ($a_2 = 92.47\%$). The fluorescence decay times of polynucleotide-free DAPI at various pH values[22] and of the DAPI−poly[d(A−T)$_2$] complexes have been reported.[23] Although the results from the three-component analysis agree with reported results, neither residuals nor the χ^2 value improved by the three-component analysis compared to the two-component analysis in our conditions. One decay time, approximately 4 ns, for DAPI bound to AT polynucleotide was also reported, obtained using the phase modulation technique.[21c] However, in our case, one-component analysis resulted in a $\chi^2 = 2.42$, which was improved to $\chi^2 = 1.12$ for two-component analysis. Therefore, the results from two-component analysis will be used for further discussion. In the presence of TMPyP, both the long decay time and its amplitude tend to decrease. For instance, the long decay time of the DAPI−poly[d(A−T)$_2$] complex is 3.07 ns, with its relative amplitude at 63.91% (Figure 8a, curve 4). A Stern−Volmer type plot of the ratio of the average decay time in the absence of TMPyP to that in its presence is depicted in Figure 8b. For two-component analysis,[17] the average decay time is defined by $\tau = (a_1\tau_1^2 + a_2\tau_2^2)/(a_1\tau_1 + a_2\tau_2)$. The slope of the ratio $\langle\tau_0\rangle/\langle\tau\rangle$ versus [TMPyP] is about 0.88×10^6 M^{-1} for the DAPI−poly(dA)·poly(dT) complex and 1.21×10^6 M^{-1} for the DAPI−poly[d(A−T)$_2$] complex (Figure 8b). The bimolecular quenching rate, k_q, reflecting the efficiency of dynamic quenching or the accessibility of the fluorephores to the quencher, 2.24×10^{14} and 3.14×10^{14} M^{-1} s^{-1}, is obtained by dividing the measured K_D by the average fluorescence decay time τ_0 of the polynucleotide-bound DAPI in the absence of TMPyP.

Discussion

Binding Mode of TMPyP to Poly(dA)·Poly(dT) and Poly[d(A−T)$_2$]. When associated with AT-rich poly- and oligonucleotides, TMPyP produces a positive CD signal in the Soret region at a low [TMPyP]/[DNA base], which has been attributed to a monomeric TMPyP, locating at or near the groove of the double helix. It has been recently reported that the positive CD signals of TMPyP when associated with duplex d(A)$_{12}$·d(T)$_{12}$ and d[(A−T)$_6$]$_2$ and with triplex d(A)$_{12}$·[d(T)$_{12}$]$_2$ are similar.[8,9] These observations indicate that TMPyP binds at the minor groove of the AT-rich oligonucleotides, since thymines have been known to be at the major groove in triplex DNA, thereby blocking or alternating the binding properties of the major groove binding drugs.[24] Given this result, the question that remains is whether the crescent-shaped side of the TMPyP that matches the turn of the helical motif in DNA fits deep into the minor groove. The spectral properties, including the normal absorption spectrum and CD, of the DAPI−poly(dA)·poly(dT) complex and the DAPI−poly[d(A−T)$_2$] complex essentially do not change even when TMPyP is bound simultaneously at high binding densities, indicating that the replacement of DAPI by TMPyP did not occur. The spectral properties of TMPyP in the presence and in the absence of DAPI are also similar. This observation indicates that DAPI and TMPyP simultaneously bind at the minor groove of AT-rich double-helical DNA. The ratio of the concentrations [DAPI]/[DNA base] is 0.08, corresponding to six base pairs per DAPI molecule, at which DAPI has been known to nearly saturate the minor groove.[11] The ratio [TMPyP]/[DNA base] is 0.05, corresponding to 10 base pairs per TMPyP. The angle between the two transitions of DAPI and the DNA helix axis has been determined as 40−45° by analyzing the LD^r spectrum.[11] The angles of DAPI transition relative to the DNA helix axis are 40−41° for the DAPI−poly(dA)·poly(dT) complex and 40−44° for the DAPI−poly[d(A−T)$_2$] complex, which are in agreement. In the presence of TMPyP, the magnitude of LD^r in the DAPI absorption region decreases, resulting in angles of 48−49° for the DAPI−poly(dA)·poly(dT) complex and 50−51° for the DAPI−poly[d(A−T)$_2$] complex. The change in angle may be the result of the negative contribution of TMPyP in the DAPI absorption region and of DNA bending: DNA bending upon TMPyP binding can be noticed by the decrease in LD^r in the DNA absorption region, i.e., by comparison of LD^r of the drug-free polynucleotide and the TMPyP−polynucleotide complex (Figure 5).

(22) Szabo, A. G.; Krajcarski, D. T.; Cavatorta, P.; Masotti, L.; Barcellona, M. L. *Photochem. Photobiol*. **1985**, *44*, 143−150.

(23) (a) Cavatorta, P.; Masotti, L.; Szabo, A. G. *Biophys. Chem*. **1985**, *22*, 11−16. (b) Barcellona, M. L.; Gratton, E. *Biochim. Biophys. Acta* **1989**, *993*, 174−178. (c) Barcellona, M. L.; Cardiel, G.; Gratton, E. *Biochem. Biophys. Res. Commun*. **1990**, *170*, 270−280.

(24) (a) Kim, S. K.; Nordén, B. *FEBS Lett*. **1993**, *315*, 61−64. (b) Tuite, E.; Nordén, B. *J. Chem. Soc., Chem. Commun*. **1995**, 53−54.

TMPyP possesses two degenerate in-plane electric transitions which are perpendicular to each other (Figure 1). Upon binding of TMPyP to DNA, the degeneracy of the transition moments of porphyrin in the Soret band (B_x and B_y bands) is removed as a result of having different angles with respect to the DNA helix axis.[5] From this assumption, angles of 55° and 70−80° between the transition moment of TMPyP and the DNA helix axis are obtained for both the TMPyP−poly(dA)·poly(dT) and TMPyP−poly[d(A−T)$_2$] complexes. These angles give additional evidence against the binding mode in which the side of the TMPyP fits into the minor groove: the angle is 45° between the TMPyP transitions and the DNA helix axis; therefore, a positive, wavelength-independent LD^r signal would be expected in the Soret absorption region for this binding mode.

Rejection of the possibilities of the major groove binding and the classical minor groove binding, and the fact that the presence of DAPI did not significantly alter the spectral properties of TMPyP, leaves us one possible binding mode for TMPyP, in which TMPyP binds across the minor groove of DNA (Figure 9). The distance between the positive charges on the porphyrin that are next to each other was estimated as 11 Å, and that across the porphine ring was 15 Å. The distance between phosphates on the opposite strands was estimated as 18 Å. However, the distance to the phosphate group three bases away on the opposite strand was 12 Å, leading us to conclude that the positive charges of the porphyrin conceivably interact with the phosphate group that is three bases away. As shown in the scheme, the coexistence of DAPI and TMPyP on AT-rich polynucleotide does not alter the essential binding properties of the each.

Energy Transfer from DAPI to TMPyP. A decrease in the fluorescence intensity of the DAPI−polynucleotide complex by TMPyP indicates the occurrence of the energy transfer from the excited state of DAPI to TMPyP. A large overlap between the emission band of the DAPI complexed with polynucleotide and the absorption spectrum of TMPyP−polynucleotide complex indicates that the mechanism behind the decrease in DAPI fluorescence involves, at least in part, the resonance energy transfer type. However, the sphere radii near 125 and 122 Å, which are calculated from our results, suggest that the efficiency of the fluorescence quenching is far higher than that for the simple complex formation. The electronic charges of the quenchers can increase the quenching efficiency dramatically. The quenching may be more efficient for the positively charged quenchers in the high negative charge density of DNA. For instance, the fluorescence of ethidium ion is effectively quenched by cationic porphyrins in the presence of DNA.[21] This result has been assigned to a long-range energy transfer.

The diffusion-controlled quenching typically results in values of the bimolecular quenching constant, k_q, near 1×10^{10} M^{-1} s^{-1}. Smaller values of k_q can result from steric shielding of the fluorophore from quencher, while larger apparent values of k_q usually indicate some type of binding interaction.[17] The k_q values of 2.24×10^{14} and 3.14×10^{14} M^{-1} s^{-1}, respectively, in the presence of poly(dA)·poly(dT) and poly[d(A−T)$_2$] are far higher than the usual bimolecular quenching constants. This result may be understood on the basis of the fact that both DAPI and TMPyP nearly bind at the minor groove of polynucleotide; therefore, the chances of collision between them are far higher compared to those of diffusion-controlled collision. A similar behavior with a 5−10 times lower k_q was reported for the DAPI−Ru(II) complex−AT-rich polynucleotide system, in which the Ru(II) complex is intercalated from the major groove.[25]

Acknowledgment. This work was supported by the Korea Research Foundation (Grant No. KRF 2002-070-C00053).

JA044555W

(25) Lee, B. W.; Moon, S. J.; Youn, M. R.; Kim, J. H.; Jang, H. G.; Kim, S. K. *Biophys. J.* **2003**, *85*, 3865−3871.